

Direct Metal Laser Re-Melting of 316L Stainless Steel Powder

Part 2: Analysis of Cubic Primitives

Rhys Morgan, Adam Papworth, Chris Sutcliffe, Pete Fox, Bill O'Neill

Research in Advanced Technologies Group

Faculty of Engineering, The University of Liverpool, UK.

Abstract

The paper reports the production of cubic primitives by Direct Metal Laser Re-Melting (DMLR) a process variant of Selective Laser Sintering. Stainless steel powder fractions are melted and fused by a high power Nd:YAG laser in a room temperature, inert environment. Research in DMLR has paid particular attention to the Q-switch pulsed laser interaction with the powder bed. High peak powers (as a result of controlling Q-switch pulse repetition frequencies) cause vaporisation and re-distribution of the melt through recoil forces acting towards the powder layer. Through a variety of density measurements, cubes have exhibited densities between 30% and 89%. Results show that in certain lasing regimes, Q-switch pulsing within a certain frequency range can yield increased densities compared with Continuous Wave (CW) produced samples. The results also show, in terms of the Andrew Number, the effect of scan speed and scan spacing on part densities. Optical analysis of porosity has exposed angular, periodic porosity in the plane normal to the scan direction and random porosity along the scan direction. Causes of this and methods of its removal are discussed. Scan strategies have been developed to produce densities in excess of 99%.

Introduction

Research in Rapid Prototyping (RP) technologies is moving towards the development of processes that will enable tool-less Rapid Manufacturing. A significant drawback to the success of these processes gaining popularity in a mass-manufacturing environment, is the lack of adequate materials characteristics of components compared with traditional manufacturing processes (*i.e. machining operations, injection molding etc*). Particularly, in the case of Selective Laser Sintering of metal parts, the density and hence mechanical characteristics of components produced by the process, is in question. Current commercial systems require the use of mechanically inferior alloys with low melt temperatures to effect densification by improved wetting during the process, or infiltration following the process. Thus the components produced will never achieve the same mechanical or material characteristic as those produced conventionally.

A number of research institutions and companies alike, have been investigating the possibility of direct laser fusion of single component powders with a view to achieving full density, high

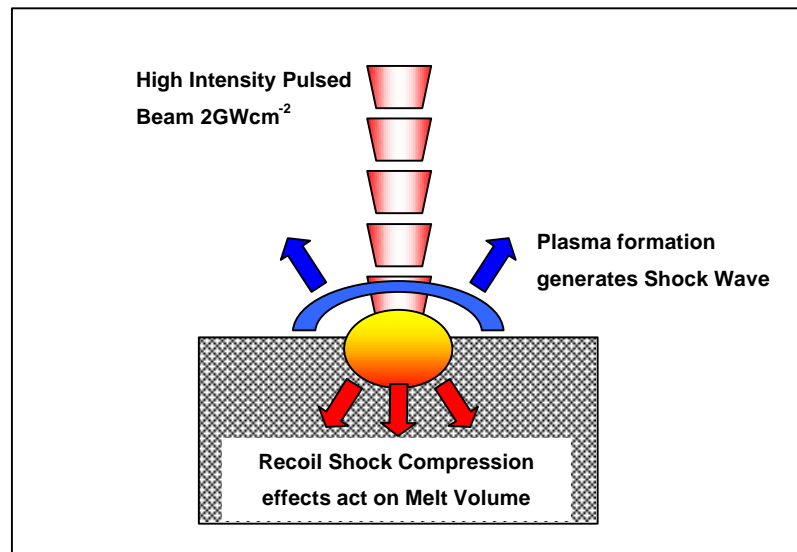


Figure 1: Interaction of Pulsed Laser with Powder Bed

mechanical strength parts for heavy duty industrial use, without the requirement of binders or infiltrants. There exist significant problems with such systems, particularly with melt dynamics and high temperature oxidation (Meiners 1997; Hauser, 1999). The existence of large thermal gradients inherent in laser sintering processes has been previously reported (Deckard 1995). These reduce the wetting characteristics of the melt and also lead to thermal stresses in the solidified layers, causing curl and deformation. Further effects of Marangoni convective flow within the melt volume cause cylindrical shaping of the melt bead (Pericleous, 1995; Lampa 1997) resulting in areas of porosity between scan lines. High temperature oxidation of the re-solidified powder layer also reduces wetting and can prevent bonding between layers (Carter, 1993). A fundamental problem arises with density of components in pre-placed powder processes such as these due to the inherent low density of the powder bed.

It has been argued that, as interaction times are several orders of magnitude shorter in SLS than in conventional sintering processes, rearrangement of particles in liquid phase sintering is essentially the only operative densification mechanism (Karapatis 1999). However, this assumes a partial melting of the powder layer. In order to achieve the mechanical characteristics of conventionally manufactured components, full melting of the powder layers must be achieved.

This paper reports on research in Direct Metal Laser Remelting (DMLR), utilising high power Nd:YAG laser to achieve full density components. The research has investigated, in particular, the effects of pulsed laser interaction with the powder bed.

Pulsed Laser Interactions

Pulsed lasers have been used in a variety of process to utilise the non-thermal photodisruption effects of the laser/material interaction (Asmus, 1986). Q Switching (rapid shuttering of the laser cavity) enables low energy pulses to be emitted over nanosecond timescales. With small beam diameters, this generates Peak Power Densities in excess of 2GWcm^{-2} (Sano, 2000). The material quickly melts and evaporates. The fast expanding vapour ejected from the surface produces a shock wave, which propagates radially from the interaction area. This causes a recoil force to impinge on the liquid substrate as shown in Figure 1. This has been shown, in laser welding, to overcome Marangoni forces acting on the melt volume (Ohmura, 1997). These effects have been investigated in DMLR with a view to overcoming the forces acting on the melt, to form a flatter, wider profile of the melt bead so as to increase final part density.

Experimental Arrangement

The experimental test facility consists of a Rofin Sinar 90W, Q-Switched, flash lamp pumped, Nd:YAG Industrial Laser Marker. Pulse Repetition Frequencies (PRF) are in the range 0 – 60kHz, where 0kHz is Continuous Wave (CW) mode. Pulse energies and pulse widths are in the range 1-30mJ and 80-200ns respectively. Maximum output power is measured at 80W with a minimum beam diameter of $100\mu\text{m}$. Scanning is accomplished by an integrated galvo-scanner head over an 80mm^2 area, where scan speeds up to 500mms^{-1} can be achieved.

The build chamber has been constructed in-house; it is typical of SLS build chambers. The chamber has a single powder feed cylinder. Platform control is by way of linear stepping actuators, controlled by pc based microstep controller, to enable $1\mu\text{m}$ linear step size. A counter-rotating roller is used to deposit powder over the build area. The whole system is enclosed in an atmospheric control chamber to enable evacuation of atmosphere and refill with inert process gas. The system is controlled by in-house software, which provides full communication and automation between laser and process chamber.

Gas atomised, austenitic stainless steel 316L was used during the study. The powder is generally spherical in form and has a wide distribution. Particle diameters are in the range $<1-56\mu\text{m}$ with 80% $<22\mu\text{m}$. The elemental composition of the alloy powder is: 16.73Cr, 13.19Ni, 0.017C, 0.71Si, 2.69Mo, 1.69Mn, Fe bal. The powder bed was measured for density by fabricating a hollow box on a stainless steel plate using the DMLR process. The insides of the box being filled with the unmelted loose powder delivered to the build area. This gave a realistic assessment of the density as the powder was deposited into the box (layer by layer) in exactly the same way as the

Laser / Scanning Parameter	Values
Average Power, P (W)	80W Constant
Pulse Repetition Frequency, f (kHz)	10, 20, 30, 40, 50, 60
Scan Speed, v (mms ⁻¹)	50, 100, 200, 300, 400, 500
Scan Spacing, s (%)	25, 50, 75, 90, 100, 110, 125

Table 1: Laser / Scanning Parameter Ranges

powder was deposited for the cube fabrication during for the experiments. Three measurements of powder bed density were taken with the average density being recorded as 48% of full density.

Experimental Procedure

Cube Fabrication

Preliminary studies on loose powder beds revealed an increase in volume of the melt tracks during the scanning of the first line compared with the rest of the layer, which produces First Line Scan Balling (Hauser 1999, Morgan 2001). To overcome this effect, all cubes were built on a substrate plate of 316L stainless steel.

Cubes were fabricated at a variety of scan speeds, scan spacings (the distance between two adjacent scan lines) and PRF. Due to conduction effects of the substrate, maximum power was maintained throughout the builds. The build platform was adjusted such that the beam remained at the focal position with a diameter of 100 μ m. A Nitrogen shroud gas was used during the process. Nitrogen gas has shown to reduce porosity in stainless steel in laser welding processes (Katayama, 2000). A series of seven cubes were produced during each build. Pulse frequency was varied for each cube, while the scan speed and scan spacing remained constant for each experiment. The cubes are produced with a simple bi-directional raster scan strategy with scan spacing dictating the distance between consecutive scans.

Density Measurements

Cube densities were measured by two methods. The first was a simple mass/volume measurement. Mitutoyo digital callipers (500-171) were used to measure five points for x,y,z measurements, while mass was measured by digital balance (Oertling RB300, to 4 decimal places). The second method of density analysis was by Xylene impregnation technique (Arthur 1954). The cubes are immersed in xylene and placed under vacuum. The xylene is impregnated into interconnected pores during this process. Following the evacuation, the samples are weighed in air and water. The xylene, being non-miscible in water, does not allow it to penetrate into the

open pores. The respective densities of xylene and steel are known, and therefore, the difference in weighting using given formulae enable open, closed and total porosity to be calculated.

Samples were prepared for optical examination by typical metallographic techniques. A simple histogram technique was used on b/w images for optical analysis of density (for cross-reference purposes), however optical analysis was mainly concerned with pore shape and size.

Results and Discussion

Density Measurements

Figure 2 shows a typical set of density measurements of cubes produced at 80W and with 75 μ m Scan Spacing, measured by mass/volume and xylene impregnation techniques. The two sets of have good correlation, with the xylene technique providing slightly higher values. Measurements in the Mass/Volume technique accounts for the inaccuracies as the cubes were not square.

The graphs show the effect of pulse frequency on the resulting density of the samples. CW mode and high PRF lasing regimes produce the highest densities at 89%. There is a significant reduction of the resulting part density at 10-20kHz pulse frequency. This is due to the detrimental effects of the high peak powers as the beam impacts the powder bed; the plasma formed during the illumination of the bed and its resulting shock wave visibly blasts powder from the interaction site. The density of samples produced at the higher speeds (400-500mms⁻¹) are actually less than the loose powder bed density. Cube density continues to increase throughout the 30-40kHz

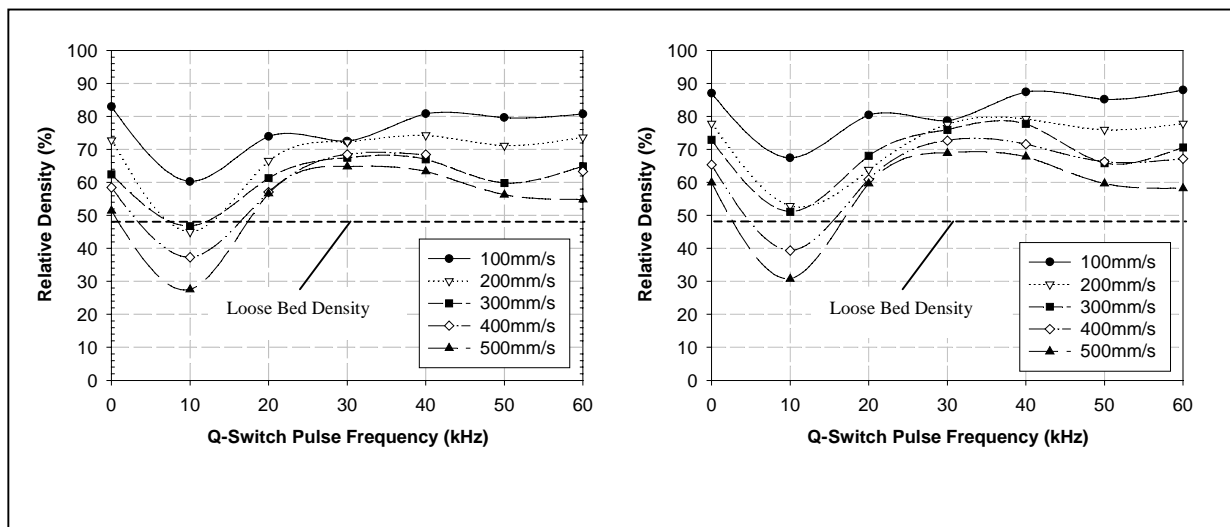


Figure 2: Density Measurements of DMLR Cubes produced at 80W Average Power and 75 μ m Scan Spacing by Mass/Volume and Xylene Impregnation Techniques

range, and at high pulse frequencies (>50kHz) the resulting densities are very similar to those produced during the CW lasing regime.

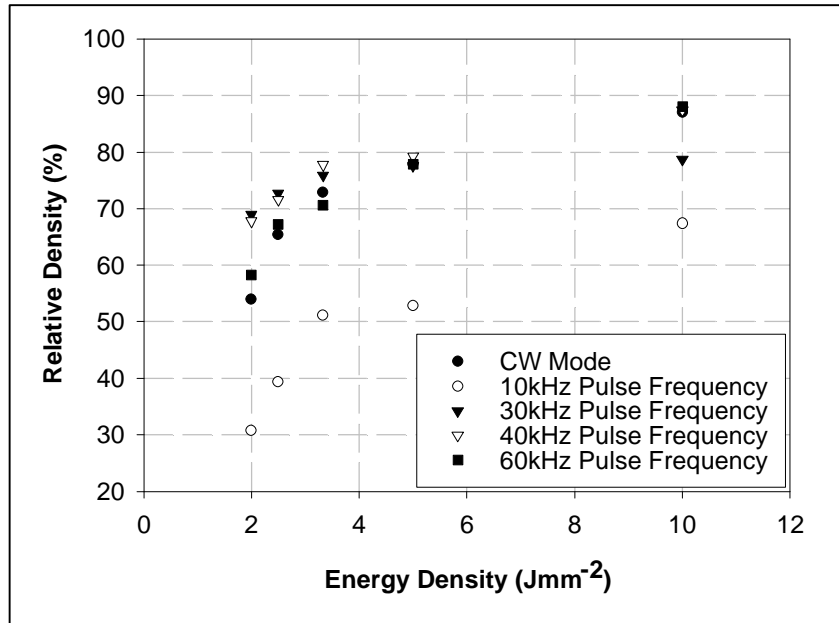


Figure 3: DMLR Cube Density as a function of Andrew Number (Energy Density)

A clearer view of the effect of scan speed and scan spacing is achieved when representing the results in terms of the Andrew number (Jmm^{-2}); a measure of the total incident energy density of a layer scan: $A_N = P / vd$, where: P, Power (W), v Scan Speed (mms^{-1}), d Scan Spacing (mm). Figure 3 shows density as a function of Andrew Number for varying pulse frequencies. At high scan speeds and large scan spacing (i.e. low Andrew Number), the results show an increase in part density for pulse frequencies in the range 30-40kHz, compared with CW and 60kHz PRF. As energy to the powder layers is increased (by reduction in speed), the overall densities of the cubes increase. The CW and 60kHz PRF cubes now exhibit the greatest density. Any further increase in energy density beyond $10Jmm^{-2}$ does not yield increased cube density. Reductions in scan speed to $50mms^{-1}$ for a scan spacing of $25\mu m$ resulted in excessive heat input to the build layers causing deformation of the layers and failure of the build.

Figure 4 shows the effect of scan spacing on part density. The results show that; at high scan speeds, the part density decreases with increasing scan spacing. However, at low scan speeds, this effect is reduced and, at $100mms^{-1}$, the resulting part density increases with scan spacing. Additional cubes were produced with further reduction in scan spacing, to the point where there

was negative overlap between consecutive scan lines. At 110 μm Scan Spacing, the density is at a maximum 92% at 110 μm and decreases at 120 μm scan spacing, or -20% scan overlap.

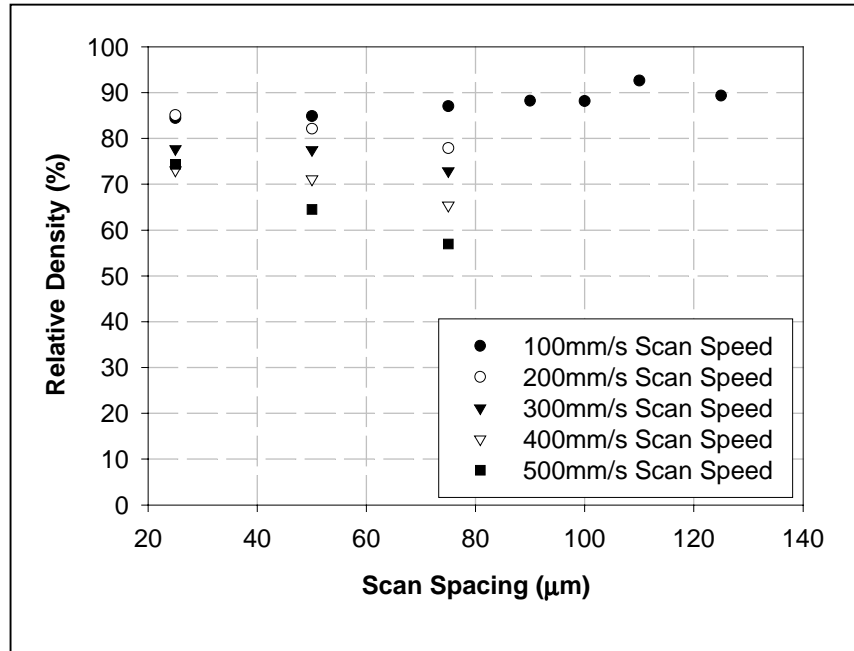


Figure 4: DMLR Cube Density as a Function of Scan Spacing(Beam Diameter 100 μm)

Optical Analysis

Optical analysis of the samples supports, qualitatively, the findings of the density measurements. Figures 5 and 6 show cross sections of samples produced at the varying laser parameters. The images show cross sections in two planes: normal to the laser scan direction and in line with the scan direction. Figure 5a-c shows the cubes produced in CW mode. The in-plane sections show diagonal porosity occurring across many layers, while the sections normal to the scan direction exhibit random porosity. The extent of porosity increases with decreasing scan spacing and increasing scan speed. The cube produced at 500 mms^{-1} reveals a flash melting of the powder bed. The diagonal porous structure is still visible. The phenomenon of angular porosity also occurs in the pulsed samples. Figure 6a-c shows sections of cubes produced at a variety of pulse frequencies and scanning parameters. The 60kHz pulsed sample displays the angular voids very prominently in the plane of scan direction. The areas of material exhibit smooth undersides, while their upper surfaces appear circular or spherical. The 30kHz sample produced at 500 mms^{-1}

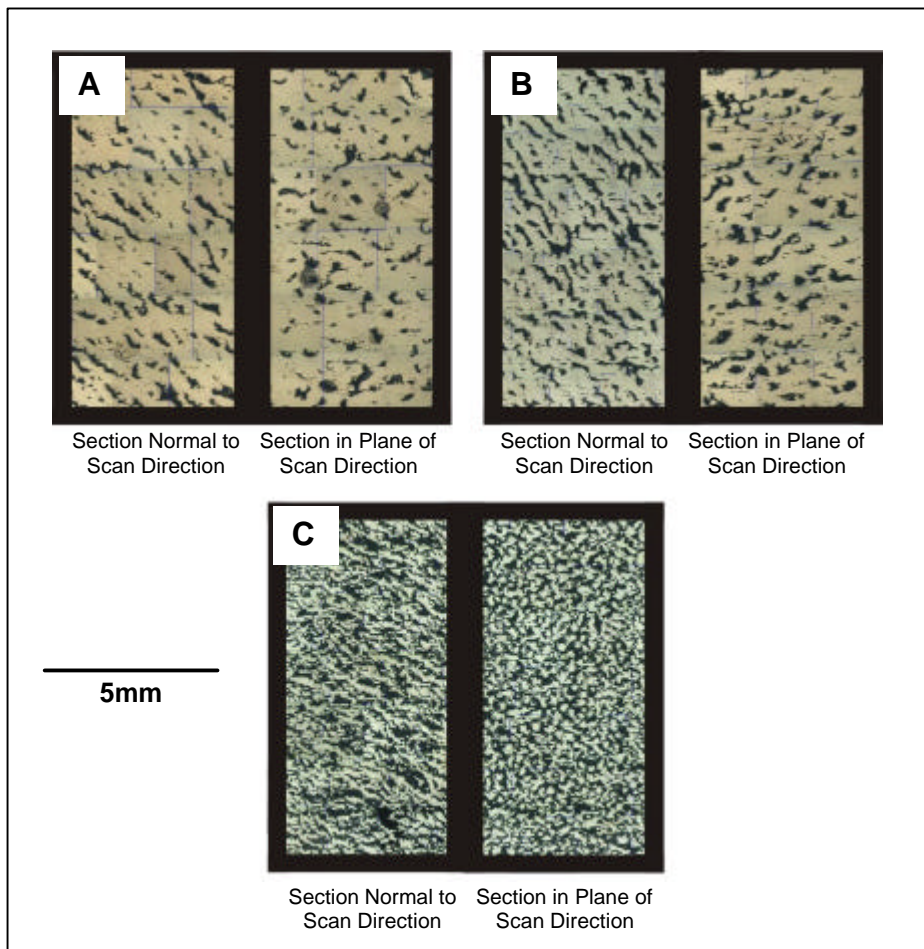


Figure 5: a) 80W, CW, 100mms^{-1} , $75\mu\text{m}$ Scan Spacing
 b) 80W, CW, 100mms^{-1} , $50\mu\text{m}$ Scan Spacing
 c) 80W, CW, 500mms^{-1} , $75\mu\text{m}$ Scan Spacing

demonstrates, like the CW sample, the effect of flash melting. However, the extent of porosity is certainly less. Figure 6c shows the cube produced at 10kHz pulse frequency. The sections show large, flat areas of melt in each layer, but very little inter-layer bonding. This occurs in both sections of the sample.

The cause of angular porosity is attributed to a diagonal wave pattern (as a result of melt dynamics) visible on single scan-line thin wall structures as discussed in part 1 of this paper (Morgan, 2001). The pattern produces a roughness to the wall. When two adjacent walls are produced, the periodic roughness of the adjoining scan lines causes porosity corresponding to the angular pattern.

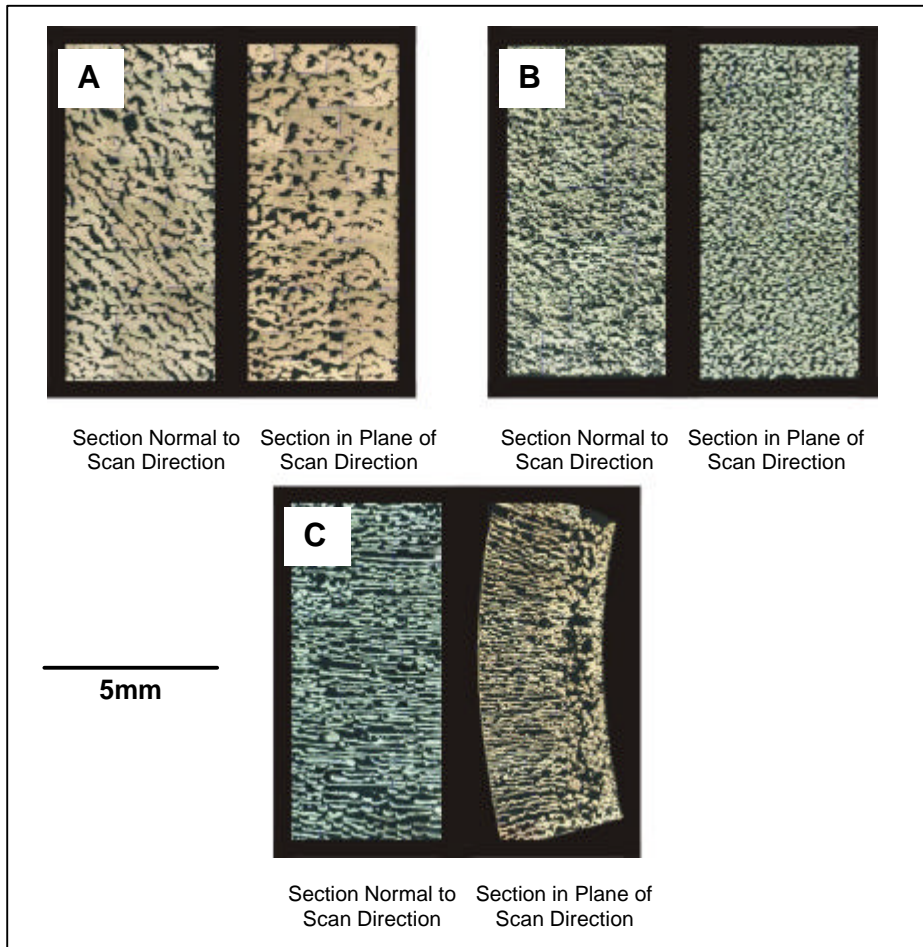


Figure 6: a) 80W, 60kHz Pulsed, 100mms⁻¹, 50mm Scan Spacing
 b) 80W, 30kHz Pulsed, 500mms⁻¹, 75mm Scan Spacing
 c) 80W, 10kHz Pulsed, 100mms⁻¹, 75mm Scan Spacing

Scan Strategies

Scan strategies were developed to remove the angular structure from the walls, in an effort to increase part density. From the previous results for optimum density, laser power and scan speeds were set at 80W and 100mms⁻¹ respectively. The laser was run in CW mode. The scan strategy involved the creation of a bi-directional rasterscan tracks, whose widths were less than that of the periodicity of the wave formation; a 0.75mm scan length was chosen. The scan spacing between successive scan lines in a track was varied and optimised at 115µm for a 100µm beam diameter, thus creating a negative (-ve) 15% overlap (Figure 7a).

Trials were undertaken to devise optimum quilting strategies. It was found that regardless of overlap between adjacent rasterscan tracks, porosity remained in the solidified layers due to the inherent lack of powder in the low-density bed. The strategy was modified such a powder refill cycle was introduced between the scanning of alternate odd/even tracks, as illustrated in figure 7.

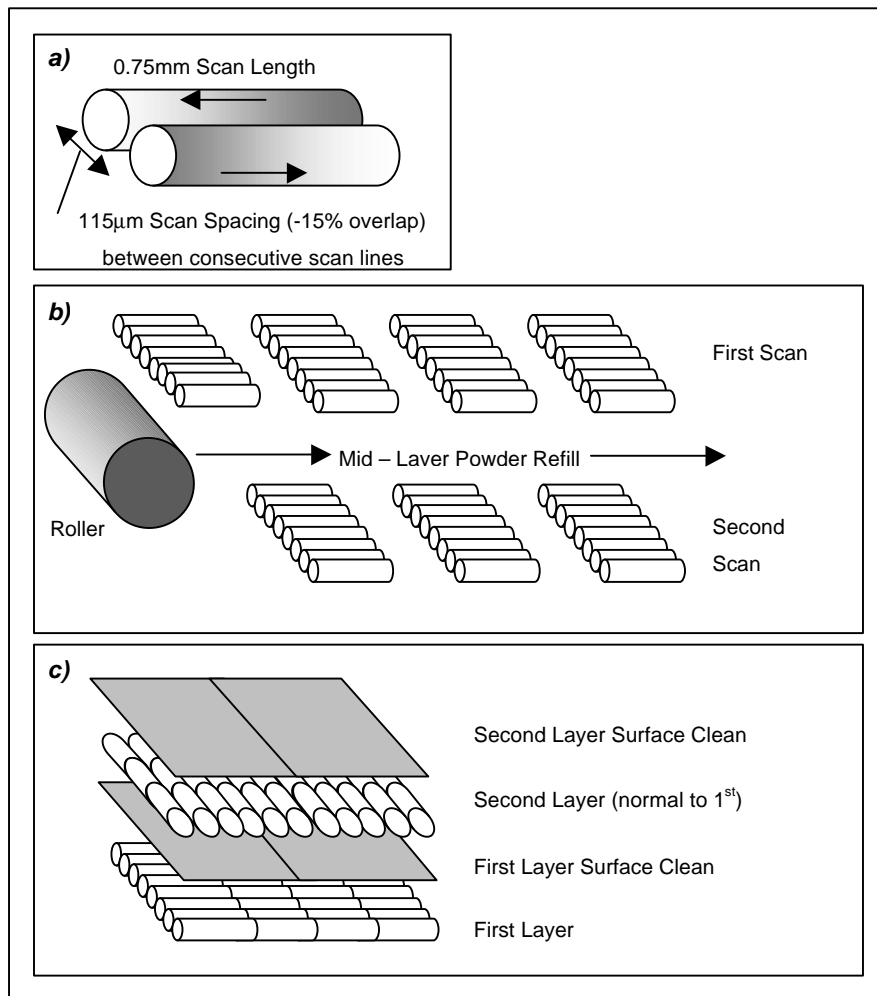


Figure 7: Scan Strategy for Production of >99% Dense DMLR Cube

- a) Two consecutive Scan Lines,
- b) Construction of a Single Layer
- c) Multiple Layers inc. Cleaning Process Steps

The powder refill cycle increased density, measured by optical analysis, to 98%. However, interconnected porosity remained across several layers. The cause of the voiding was attributed to gas entrapment upon deposition of new layers on rough laser re-melted surfaces. The strategy was further developed to scan each layer normal to the preceding layer to avoid interconnected porosity (Figure 7c). An additional cleaning step was introduced to scan over the re-solidified surface to reduce surface roughness. Minimal re-melting takes place due to the reduced absorption coefficient of the highly reflecting surface.

Though the addition of powder refill and surface clean incur time penalties, density measurements by Xylene impregnation technique show an increase to 99.65% of full density.

With the new scan strategies, pulsed mode is being investigated, and further developments to the scan strategy are currently being undertaken to reduce the build time. Figure 8 shows a polished cube produced by the DMLR technique.



*Figure 8: Stainless Steel 316L Cube Produced by DMLR
(Density >99%)*

Conclusions

The work has shown the development of the DMLR process as a one-step route for the production of high-density stainless steel components. Pulsed interactions with the material have shown to vary the density of cubes produced. Pulsed interactions with the powder layer have shown to be beneficial for certain parameters, though CW mode scanning has produced the greatest density. Certain pulse repetition rates are detrimental as shock waves blast the powder from the bed. There is a strong possibility that pulsed scanning may enable graduated porosity in the construction of objects, this is being investigated. Optical analysis of cross sections of the cubes revealed periodic diagonal porosity throughout the samples. This is attributed to melt dynamics and observed on thin wall structures. To remove the porosity, scan strategies were developed, resulting in part densities in excess of 99%.

Acknowledgments

The authors would like to thank Mr Lawrence Bailey, experimental officer, for the construction of the experimental apparatus. Rhys Morgan is approaching the culmination of his PhD research and would like to take this opportunity to thank the other authors and Mr Bailey for their continued support and efforts during the project.

References

- Meiners, W., Wissenbach, K., Propawe, R.,** Direct Selective Laser Sintering of Steel Powder. Laser Assisted Net shape Engineering 2, Proc. LANE 1997 pp. 615-622
- Hauser, C., Childs, T.H.C., Dalgarno, K.W., Eane, R.B.,** Atmospheric control during Selective Laser Sintering of Stainless Steel 314S Powder. Proceedings of the Solid Freeform Fabrication Symposium, University of Texas at Austin, Texas. Vol. 10, pp. 265-272
- Deckard, C., Miller, D.,** Improved Energy Delivery for Selective Laser Sintering Proc Solid Freeform Fabrication Symposium. The University of Texas at Austin, Texas. Vol. 6. 1995 pp. 151-158
- Pericleous, K. A., Bailey, C.,** Study of Marangoni phenomena in laser-melted pools Meeting: Proc 1995 7th Conf Model Casting Welding Adv Solid Process, Sep 10-15 1995
- Lampa, C., Kaplan, A. F. H., Powell, J., Magnusson, C.,** Analytical thermodynamic model of laser welding Journal of Physics D: Applied Physics, Vol. 30, No. 9, (May 7 1997), pp. 1293-1299
- Carter, W.T., Jones, M. G.,** Direct Laser Sintering of Metals. Proc Solid Freeform Fabrication Symposium. The University of Texas at Austin, Texas. Vol 4. 1993 pp. 51-59
- Karapatis, N.P., Egger, G., Gygax, P.E., Glardon, R.,** Optimisation of Powder Layer Density in Selective Laser Sintering Proceedings of the Solid Freeform Fabrication Symposium, University of Texas at Austin, Texas. 1999 pp. 255-263
- John Asmus** More light for art conservation IEEE Circuits and Devices Magazine No. 2, Vol. 2. 1986 pp. 6-15
- Sano, Y., Kimura, M., Mukai, N., Yoda, M., Obata, M., Ogisu, T.,** Process and application of shock compression by nano-second pulses of frequency doubled Nd:YAG laser. Proc. SPIE 2000, (3888) pp. 294-306
- Ohmura, E., Hayashi, H., Fujimori, S., Miyamoto, I.,** Thermohydrodynamics Analysis of Fusion Phenomena Accompanied with Evaporation due to Laser Irradiation. Proc. LIA ICALEO 1997. Section G pp.9-15
- Morgan, R., Sutcliffe, C.J., O'Neill, W.,** Experimental Investigation of nanosecond pulsed Nd:YAG laser Re-Melted Pre Placed Powder Beds. Rapid Prototyping Journal Vol. 7, No. 3, 2001

Katayama, S., Seto, N., Mizutani, M., Matsunawa, A., Formation mechanism of porosity in high power YAG laser welding. Proc. ICALEO 2000, Section C pp. 6-24

Arthur, G., Porosity and permeability changes during the sintering of copper powder. Journal of the Institute of Metals 1954-55 (83) pp. 329-336

Rhys Morgan, Adam Papworth, Chris Sutcliffe, Pete Fox, Bill O'Neill, Direct Metal Laser Re-Melting (DMLR) of 316L Stainless Steel Powder Part 1: Analysis of Thin Wall Structures. Proceedings of the Solid Freeform Fabrication Symposium, University of Texas at Austin, Texas. (Submitted 2001)